

## Seismic Active Earth Pressure of Narrow Geosynthetic-Reinforced Backfill on Rigid Facing

Fariborz Dehghani, Hadi Shahir<sup>\*</sup>, Ali Ghanbari;  
Civil Engineering Department, Faculty of Engineering, Kharazmi  
University, Tehran, Iran

Received: 17 Jan 2016

Accepted: 10 June 2016

### Abstract

In the narrow geosynthetic-reinforced retaining walls a stable rear wall exists in a short distance and there is not enough space to extend appropriate length of reinforcements. In this case, the probability of overturning of retaining wall increases especially when subjected to earthquake loading. To increase the stability of the wall, reinforcements may be connected to the stable rear surface. Alternative solution is the utilization of full-height cast in-place concrete facing in order to resist the earth pressure by combined actions of reinforcements pullout capacity and facing flexural rigidity. One of the main questions about this type of walls is the portion of earth pressure resisted by the facing. In this study, the seismic earth pressure of narrow geosynthetic-reinforced backfill on rigid facing was evaluated using limit equilibrium approach and horizontal slices method. The critical failure surface was assumed to extend linearly from the wall toe to the rear surface and then moves

---

<sup>\*</sup>Corresponding author      shahir@khu.ac.ir

along the interface of the backfill and rear surface up to the backfill surface. The effects of various parameters such as wall aspect ratio have been investigated. The obtained results show that the applied soil pressure on wall facing will be increased with depth in the upper part of the wall according to the Mononobe-Okabe equation, but its pattern is inversed in the lower part of the wall and it decreases until it reaches to zero at the wall toe. The results of analyses indicate that the attracted soil thrust by the facing increases with lessening of backfill width.

**Keywords:** Geosynthetic-reinforced soil wall, Narrow backfill, Full-height rigid facing, Seismic earth pressure, Horizontal slices method.

### Notation

b: width of backfill  
 c: cohesion  
 $F_{hi}$ : horizontal seismic force of the  $i^{\text{th}}$  slice  
 $F_{vi}$ : vertical seismic force of the  $i^{\text{th}}$  slice  
 H: height of wall  
 $h_c$ : height of intersection point of failure surface and rear surface  
 $h_i$ : height of the  $i^{\text{th}}$  slice  
 $H_i$ : horizontal interaction force between slices  $i$  and  $i-1$   
 K: at rest earth pressure coefficient  
 $K_h$ : horizontal seismic coefficient  
 $K_v$ : vertical seismic coefficient  
 $L_e$ : bonded length of reinforcement  
 $n_b$ : number of lower slices  
 $n_i$ : number of upper slices  
 $N_i$ : normal force of the  $i^{\text{th}}$  slice in the failure surface  
 $P_i$ : lateral earth pressure on facing in the  $i^{\text{th}}$  slice  
 $S_i$ : shear force of the  $i^{\text{th}}$  slice in the failure surface  
 $S_v$ : spacing of reinforcements  
 $T_a$ : pullout resistance of reinforcement  
 $T_i$ : mobilized force in the  $i^{\text{th}}$  reinforcement  
 $V_i$ : vertical interaction force between slices  $i$  and  $i-1$   
 $W_i$ : weight of the  $i^{\text{th}}$  slice  
 $X_{vi}$ : half length of upper side of the  $i^{\text{th}}$  slice  
 $\alpha$ : slope of rear surface  
 $\beta$ : slope of failure surface  
 $\gamma$ : unit weight  
 $\phi$ : friction angle  
 $\delta$ : friction angle between backfill and rear surface

## Introduction

Geosynthetic-reinforced retaining walls can be used for widening the upper space of existing retaining structures in urban areas or construction of retaining walls in front of steep rock hills. In these locations, a stable wall exists in a short distance, usually smaller than  $0.6H$  ( $H$ : wall height), behind the retaining wall.

Various researchers have been studied the behavior of conventional reinforced soil walls by different experimental, numerical and analytical methods [1-9]. In conventional reinforced soil walls, reinforcements are long enough to provide the required pullout resistance for the general stability of wall. If there is no enough space for construction of retaining wall with appropriate length of reinforcements, the probability of overturning increases [10]. The behavior of reinforced soil walls with narrow backfill or in other words, Shored Mechanically Stabilized Earth (SMSE) walls [11] have been considered in a number of studies [12-20].

In the case of narrow backfill, the reinforcements may be connected to the stable surface behind the backfill to increase the stability of the wall. However, as reported by Morrison et al. [17], this method is not sufficiently effective. Alternative solution, instead of connection of reinforcements to the rear surface is to place a full-height reinforced concrete facing over the geosynthetic-wrapped wall face [12,13]. Therefore, the combined tensile function of reinforcements and flexural rigidity of facing provides the general stability of the wall. In the 1980's,

researchers in Japan constructed a geosynthetic-reinforced soil wall using a rigid facing with reinforcement lengths considerably less than  $0.6H$  [10, 13]. A continuous rigid facing considerably enhances the seismic performance of geosynthetic-reinforced retaining walls [21].

Placement of the facing after the completion of reinforced soil wall has certain advantages [22], however, in the narrow walls there is not enough space to use reinforcements with appropriate length and so temporary stability during construction cannot be provided. Therefore, backfilling of reinforced soil layers and placement of concrete facing may be accomplished simultaneously.

The effect of reinforcement layers on reduction of soil pressure on retaining wall with unlimited backfill space has been studied by Ahmadabadi and Ghanbari [23]. They concluded that lateral earth pressure in reinforced soil walls is smaller than lateral earth pressure of unreinforced backfill. In this study due to the sufficient length of reinforcement, the soil pressure is mainly carried by the pullout resistance of reinforcements and therefore, the force acting on the facing is small. However, in narrow backfills owing to limited length of reinforcements, the pullout resistance of reinforcements is limited and a portion of the earth pressure can be carried by the reinforcements and the remaining part of that is attracted by the full-height rigid concrete facing.

In the current design method, the full-height rigid facing is designed to support the active earth pressure developed in an unreinforced

backfill [24]. However, because of the limited width of the backfill in narrow walls and also combined action of the facing rigidity and reinforcement's pullout capacity, the applied pressure on the facing can be significantly smaller than the active earth pressure of unreinforced backfill.

In this study, the seismic active earth pressure of narrow reinforced soil walls on full-height rigid facing has been evaluated using limit equilibrium approach and horizontal slices method.

### **Method of Approach**

The approach used in this study is limit equilibrium using Horizontal Slices Method (HSM). As the reinforcements are placed in horizontal direction, the backfill is divided into horizontal slices equal to number of reinforcements. This method was originally proposed by Shahgholi et al. [2] to analyze the seismic stability of reinforced soil walls. Nouri et al. [4,5] modified and verified horizontal slices method and employed it to evaluate the seismic stability of reinforced soil walls and slopes. Azad et al. [25] used HSM to investigate active pressure distribution along the height of a wall and calculated the angle of failure wedge in the active state. Shekarian et al. [26] determined the active static pressure on reinforced retaining walls in frictional and cohesive soils using HSM. This method was used by Ahmadabadi and Ghanbari [23] and Ghanbari and Ahmadabadi [27] to estimate the lateral earth pressure on the facing of reinforced soil walls with cohesive-frictional

backfills. In another study by Ghanbari and Taheri [28] effect of surcharge on active earth pressure of reinforced soil walls was analyzed using HSM.

In the above mentioned studies, different assumptions have been made about the internal and interaction forces of slices. In this study, all the forces acting on each slice and interaction forces between slices have been considered and the force and moment equilibrium equations were satisfied. As shown in Figure 1, the assumed failure surface starts linear from toe of the wall and continues until meeting the rear surface and then continues along the interface of the backfill and rear surface to the top of the backfill. This failure surface has been proposed in FHWA manual [11] for narrow retaining walls with extensible reinforcements. According to this manual, the suggested angle of failure surface at the bottom of the wall for backfills with flexible reinforcements is equal to  $45 + \varphi/2$ . In this study, the angle of failure surface has been considered unknown and determined by maximizing the summation of earth pressure resultant acting on the wall and the tensile forces of the reinforcements.

The free body diagrams for different slices are depicted in Figure 2. The assumed unknowns and equations are listed in Table 1. As the failure wedge consists of two parts, unknowns and equations should be written for two parts, separately. The number of slices for each part is calculated using the following equations:

$$h_c = \frac{b}{\cot\beta - \cot\alpha} \quad (1)$$

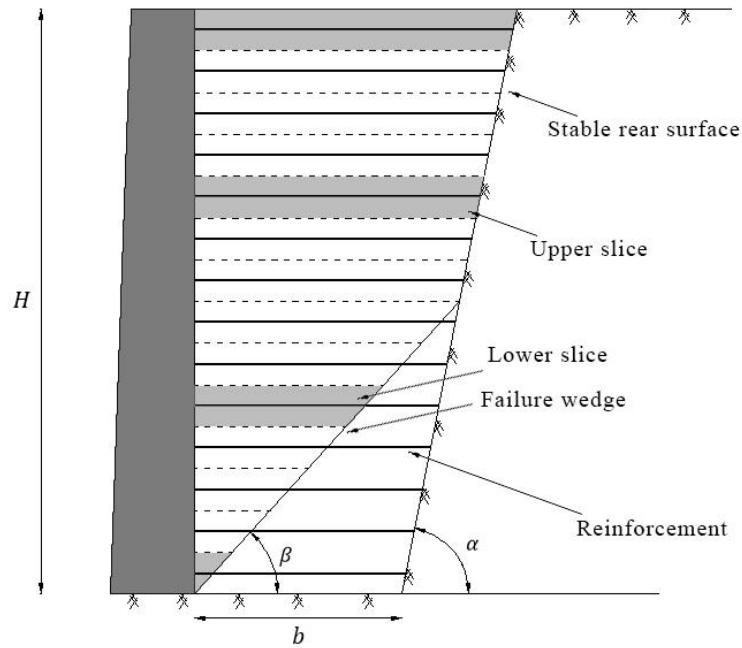


**Figure 1. Division Of failure wedge into horizontal slices**

$$n_b = \frac{h_c}{h} \quad (2)$$

$$n_t = n - n_b \quad (3)$$

where  $h_c$  is the height of the intersection point of failure surface and rear surface,  $n_b$  is the number of lower slices and  $n_t$  is the number of upper slices. The definitions of other parameters presented in Figure 1 are as follows:  $\beta$  slope of failure surface and  $\alpha$  slope of rear surface relative to the horizon,  $b$  width of the backfill and  $H$  height of the wall. The rear surface has been considered vertical and so the angle of  $\alpha$  is 90 degrees in the current study.

The vertical stress in the narrow locations obeys the arching theory

because of stiff surfaces surrounding the backfill and the limited width of the wall. The vertical interaction force between slices was calculated using equation proposed by Janssen [29]:

$$V_i = \frac{\gamma b}{K} \left( \frac{1 - \exp\left(\frac{-2KZ_i}{b \tan \delta}\right)}{2 \tan \delta} \right) \times 2X_{vi} \quad (4)$$

$$K = 1 - \sin \varphi \quad (5)$$

where  $X_{vi}$  is the half length of the upper side of each slice,  $K$  is at rest earth pressure coefficient and is the soil unit weight. The location of application of  $V_i$  has been considered on the middle of upper side of

**Table 1. Governing equations and unknowns in current study**

| Equations   | Number     | Unknowns         | Number     |
|---|------------|------------------|------------|
| $\sum F_x = 0$ for each slice                         | $n$        | $P_i$            | $n$        |
| $\sum F_y = 0$ for each slice                         | $n$        | $T_i$            | $n_b$      |
| $\sum M_o = 0$ for lower slices                       | $n_b$      | $N_i$            | $n$        |
| $S_i = N_i(\tan \varphi) + C$ for lower slices        | $n_b$      | $S_i$            | $n_b$      |
| $S_i = N_i(\tan \delta)$ for upper slices             | $n_t$      | $S_i$            | $n_t$      |
| $H_i = \lambda(V_i(\tan \varphi) + C)$ for each slice | $n$        | $H_i$            | $n$        |
| <b>Summation</b>                                      | $4n + n_b$ | <b>Summation</b> | $4n + n_b$ |



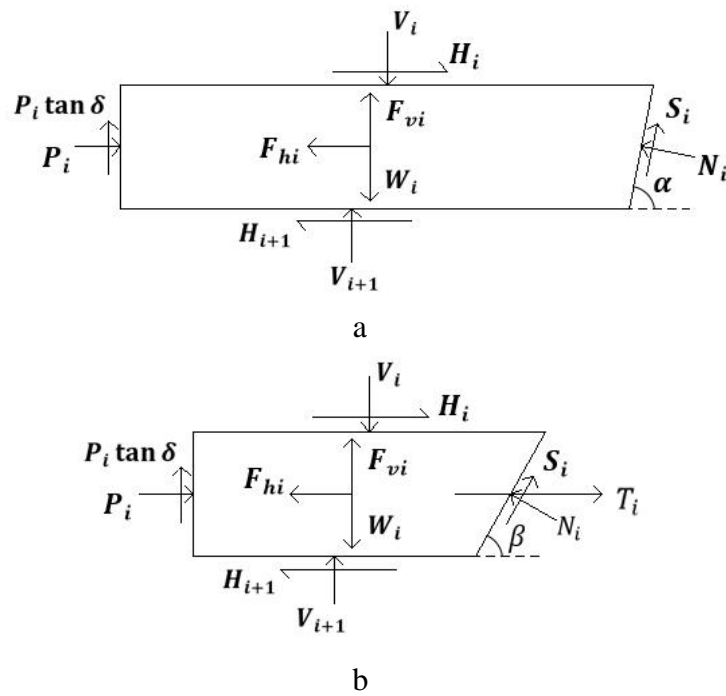


**Figure 2. Forces and loadings associated with individual slices, a) upper slices, b) lower slices**

each slice. Based on the geometry of the problem, the location of application of  $V_i$  is calculated as follows:

$$X_{v_i} = \frac{b}{2} + \frac{\sum_{j=i}^n h_j}{2 \tan \alpha} \quad \text{for upper slices} \quad (6)$$

$$X_{v_i} = \frac{\sum_{j=i}^n h_j}{2 \tan \beta} \quad \text{for lower slices} \quad (7)$$

where  $h_j$  is the height of the  $j^{\text{th}}$  slice. As given in Table 1, the horizontal interaction force between slices has been considered as a multiple of shear strength in the corresponding depth with a coefficient of  $\lambda$ . The effect of this force is negligible and some of the previous researchers neglected this force in their calculations. In this study, the value of  $\lambda$

was considered according to the charts suggested by Ahmadabadi and Ghanbari [23].

The earthquake loading has been considered by pseudo-static earthquake forces using the horizontal and vertical seismic coefficients. The earthquake forces acting on each slice are obtained.

$$F_h = K_h W_i \quad (8)$$

$$F_v = K_v W_i \quad (9)$$

where  $K_h$  and  $K_v$  are horizontal and vertical seismic coefficients, respectively and  $W_i$  is the weight of  $i^{\text{th}}$  slice.

Equilibrium equations (Equations 10 to 14) were written for each slice and the system of equations was formed. By solving the system of equations, the unknowns were determined. As the angle of failure surface has been considered unknown, using trial and error method, different values were considered for this parameter and the most critical failure surface was determined by maximizing the summation of earth pressure resultant acting on the wall and the tensile forces of the reinforcements. In the upper slices, entire length of the reinforcements is located inside the failure wedge, and in the limit equilibrium analysis, no force is mobilized. Therefore, the system of equations for the upper slices consists of two equations. In the lower slices, reinforcements have bonded length outside of the failure wedge, so the tensile force is mobilized in them and the system of equations consists of three unknowns. Governing equations for the upper slices are as follows:

$$\begin{aligned} \sum F_x = 0 &\rightarrow P_i + [\tan \delta \cos \alpha - \sin \alpha]N_i \\ &= \lambda V_{i+1} \tan \varphi - \lambda V_i \tan \varphi + F_{hi} \end{aligned} \quad (10)$$

$$\begin{aligned} \sum F_y = 0 &\rightarrow [\tan \delta]P_i + [\tan \delta \sin \alpha + \cos \alpha]N_i \\ &= W_i + V_i - V_{i+1} - F_{vi} \end{aligned} \quad (11)$$

For the lower slices the governing equations are:

$$\begin{aligned} \sum F_x = 0 &\rightarrow P_i + [\tan \delta \cos \beta - \sin \beta]N_i + T_i \\ &= \lambda V_{i+1} \tan \varphi - \lambda V_i \tan \varphi + F_{hi} \end{aligned} \quad (12)$$

$$\begin{aligned} \sum F_y = 0 &\rightarrow [\tan \delta]P_i + [\tan \delta \sin \beta + \cos \beta]N_i \\ &= W_i + V_i - V_{i+1} - F_{vi} \end{aligned} \quad (13)$$

$$\begin{aligned} \sum M_o = 0 &\rightarrow [Y_i]P_i - \left[ \frac{Y_i}{\sin \beta} \right]N_i + [Y_i]T_i \\ &= F_{hi}Y_i + \lambda V_{i+1} \tan \varphi \left( Y_i - \frac{h}{2} \right) + F_{vi}X_{G_i} + \\ &V_{i+1}X_{v_{i+1}} - \lambda V_i \tan \varphi \left( Y_i + \frac{h}{2} \right) - W_iX_{G_i} - V_iX_{v_i} \end{aligned} \quad (14)$$

According to the limited bonded length of reinforcement behind the failure wedge, the force mobilized in reinforcements should be equal to or smaller than the pullout resistance. Based on FHWA manual [11], pullout resistance of reinforcement layer is calculated using the following equation:

$$T_a = \frac{1}{FS_p} F^* \sigma_v L_e C R_c \alpha \quad (15)$$

where  $T_a$  is pullout resistance of reinforcement and  $L_e$  is bonded length.  $F^*$  is coefficient of pullout resistance which for granular soils it is considered equal to  $0.8 \tan \varphi$ .  $C$  is reinforcement effective unit perimeter that is considered equal to 2.  $\alpha$  is scale effect correction factor that is equal to 0.8 in the current problem. Coverage ratio is

presented by  $R_c$  and its value was ~~considered~~ taken equal to 1.  $\sigma_v$  is vertical stress at the depth of the reinforcement layer.  $FS_p$  is factor of safety which should be greater than 1.5.

## Results and Discussion

To study the effect of various parameters, different models were considered and analyzed using the computer code developed based on the formulation of horizontal slices method presented in the preceding sections. Variable parameters in the analyses are wall aspect ratio, internal friction angle of backfill material, horizontal and vertical seismic coefficients, vertical spacing of reinforcement layers and height of wall. Different values considered for these parameters are given in Table 2.

The results of analyses have been presented in the form of lateral earth pressure on facing (P) and mobilized tensile force in reinforcements (T) versus depth in Figure 3 to 8. Since the failure wedge consists of two parts, the obtained charts consist of two parts, too. In the upper part where the slices width is equal to the width of failure wedge, entire length of the reinforcements is placed inside the failure wedge and according to the basis of limit equilibrium method, no force is mobilized in them. Thus, ~~whole~~ the lateral earth pressure is carried out by the wall facing. However, in the lower slices reinforcements extend outside of failure wedge and a portion of lateral pressure is carried by the reinforcements. Thus, the total load is divided between reinforcements and wall facing. This leads to a jump

in the diagram of lateral earth pressure which occurs between the upper and lower parts. Also, in the upper slices the backside of slices is in contact with rear stable surface and the friction coefficient of this surface is equal to  $\tan \delta$  but in the lower slices the backside of slices is in contact with soil and hence the friction coefficient is equal to  $\tan \varphi$ . This also increases the bound between the lower and upper parts of the lateral earth pressure diagram.

**Table 2. Values of variable parameters for sensitivity analysis**

| Variable Parameter | Unit | Value          |
|--------------------|------|----------------|
| $b/H$              | -    | 0.3, 0.4, 0.5  |
| $\varphi$          | deg  | 30, 35, 40     |
| $K_h$              | -    | 0.1, 0.15, 0.2 |
| $K_v$              | -    | -0.05, 0, 0.05 |
| $H$                | m    | 9, 15          |
| $S_v$              | m    | 0.3, 0.6       |

### 1. Effect of wall aspect ratio

Variation of lateral earth pressure on facing ( $P$ ) and mobilized force in reinforcements ( $T$ ) in the height of wall for different aspect ratios (ratio of width to height of wall) are presented in Figure 3. In these graphs, wall height is equal to 9 m, internal friction angle of backfill is 30 degrees, horizontal and vertical seismic coefficients are equal to 0.2 and 0.05, respectively and vertical spacing between reinforcements is 0.3 m.

As shown in Figure 3, in the upper part of the wall the lateral earth pressure increases with depth and its rate of increase is nearly independent of wall aspect ratio. In the lower part, lateral earth pressure has a decreasing pattern and becomes zero at the toe of wall. As can be seen in this figure, the applied soil pressure on facing considerably increases by reduction of wall aspect ratio. The main reason of this observation is the reduction of reinforcements bonded length with lessening of backfill width and so the main portion of soil pressure is carried by the wall facing.

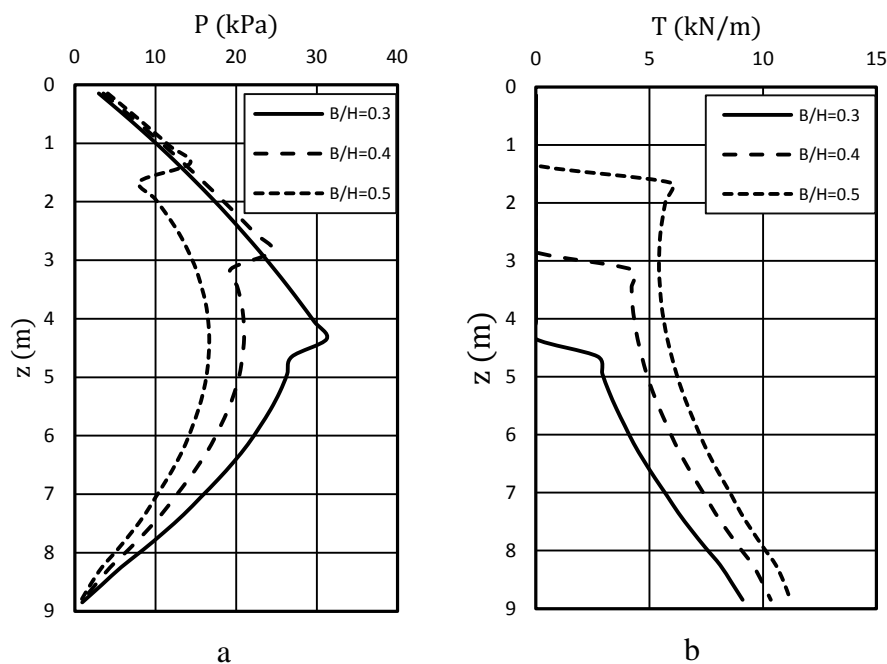


**Figure 3. Comparison of distribution of a) lateral earth pressure on facing and b) mobilized force in reinforcements for different wall aspect ratios**

Since the reinforcements only in the lower part of the wall come into action, their forces in the upper layers are equal to zero. However,

in the lower layers, considerable forces are mobilized in the reinforcements which increase with depth. The results ~~show~~ illustrate that the reinforcement forces increase with increasing of the wall aspect ratio, which is in agreement with the above mentioned concept.

## 2. Effect of internal friction angle of backfill material

Effect of the internal friction angle of backfill for a wall with height of 9 m and aspect ratio of 0.3 has been represented in Figure 4. Other parameters are the same as the aforementioned values. It is obvious that the general pattern of lateral earth pressure is similar to Figure 3. As expected, the applied lateral earth pressure on the facing and the mobilized forces in reinforcements decrease with increasing of friction angle. Also, with increasing of friction angle, the slope of failure surface increases and ~~so~~ the intersection point of the failure surface and rear stable surface is located at a higher elevation. This is clearly identified according to the location of jump in graphs of Figure 4.

## 3. Effect of seismic coefficients

The effect of horizontal seismic coefficient is ~~shown~~ depicted in Figure 5. Based on the obtained results, in the upper part of wall, the lateral earth pressure increases with increase of horizontal seismic coefficient uniformly in depth. But in the bottom part, the horizontal seismic coefficient has no effect on the lateral earth pressure. Results for the mobilized forces in reinforcements in Figure 5(b) show that the reinforcement forces increase with increase of seismic coefficient.

Since the seismic load is proportional to the weight of slices, these observations can be related to the uniform size of the upper slices and decreasing size of the lower slices with depth.

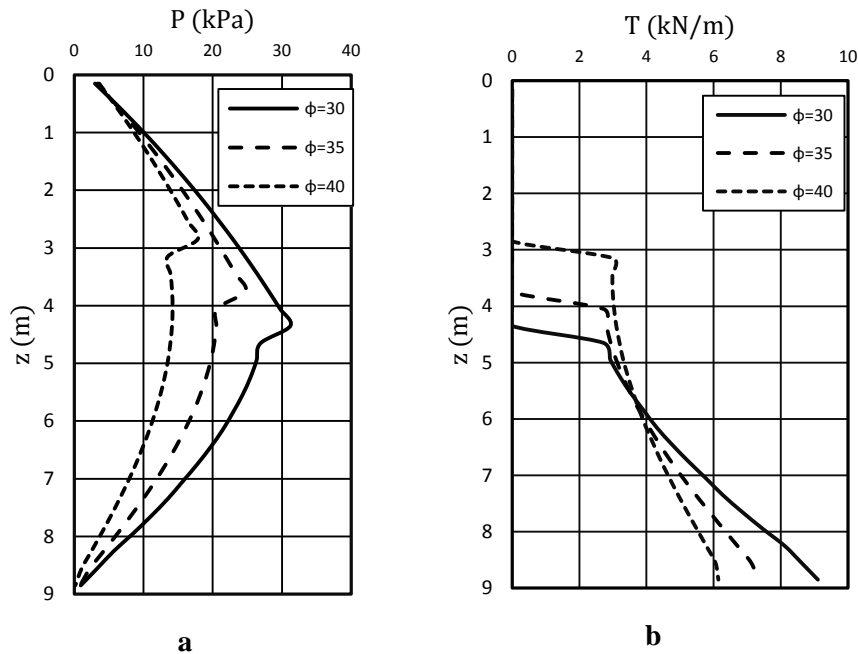


**Figure 4. Comparison of distribution of a) lateral earth pressure on facing and b) mobilized force in reinforcements for different backfill friction angles**

Effect of vertical seismic coefficient has been presented in Figure 6. Results show that negative values of vertical seismic coefficient (downward) increase the lateral earth pressure acting on the wall facing and positive values (upward) decrease it. This effect is similar in upper and middle part of the wall height, but the effect of vertical seismic loading decreases with depth and becomes negligible at the toe of wall. Thus, it can be concluded that the downward seismic loading creates more critical state regarding the lateral pressure on



wall. The results corresponding to reinforcement forces show an opposed pattern and reinforcement forces decreases with the increase of downward seismic coefficient.

#### **4. Effect of wall height and spacing of reinforcements**

In all of the preceding analyses, height of wall and spacing of reinforcements were 9 and 0.3 meters, respectively. To study the effect of these two parameters, a model with the height of 15 meters and vertical spacing of 0.3 meters and another one with the height of 9 meters and vertical spacing of 0.6 meters were analyzed. To make the results comparable, the aspect ratio of both models were considered equal to 0.3. Results for the first analysis are presented in Figure 7 and for the second one has been displayed in Figure 8.

In Figure 7 the values of lateral earth pressure and reinforcement force have been normalized by the wall height and plotted versus the normalized depth. It is observed that by normalizing the lateral earth pressure and reinforcement forces, the effect of wall height can be eliminated. This indicates that the lateral earth pressure and reinforcement forces are proportional to the wall height.

Results for different vertical spacing of the reinforcement layers are presented in Figure 8. To compare the unit force of reinforcements, the reinforcement's forces were divided by the vertical spacing of reinforcements and presented in Figure 8(b). As can be seen, the lateral earth pressure and tensile stress of reinforcements are independent of the vertical spacing of reinforcements.

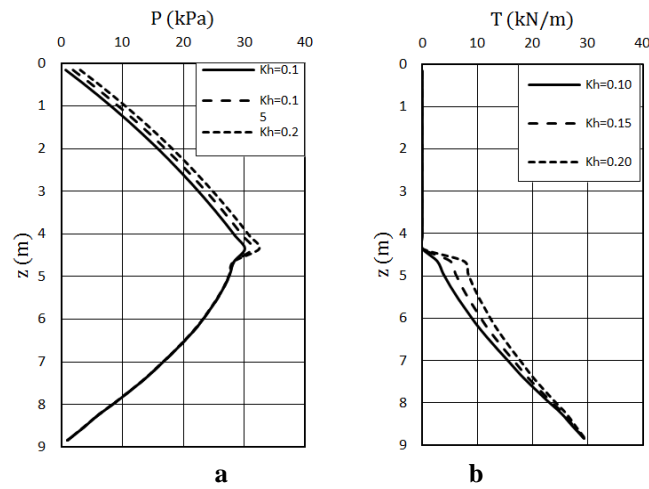


**Figure 5. Comparison of distribution of a) lateral earth pressure on facing and b) mobilized force in reinforcements for different horizontal seismic coefficient**

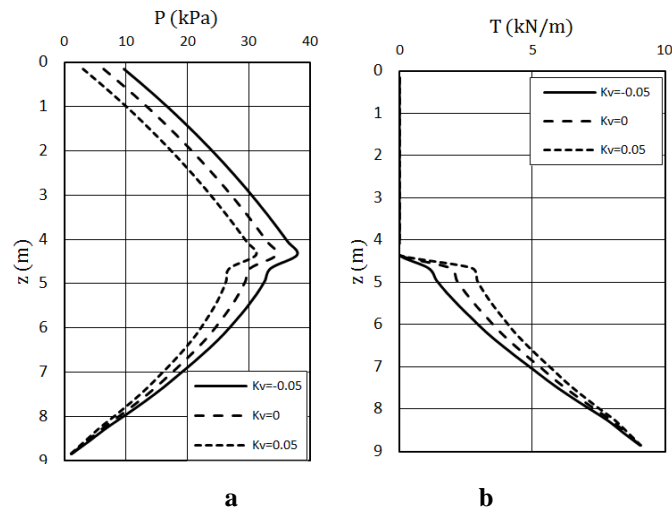


**Figure 6. Comparison of distribution of a) lateral earth pressure on facing and b) mobilized force in reinforcements for different vertical seismic coefficient**

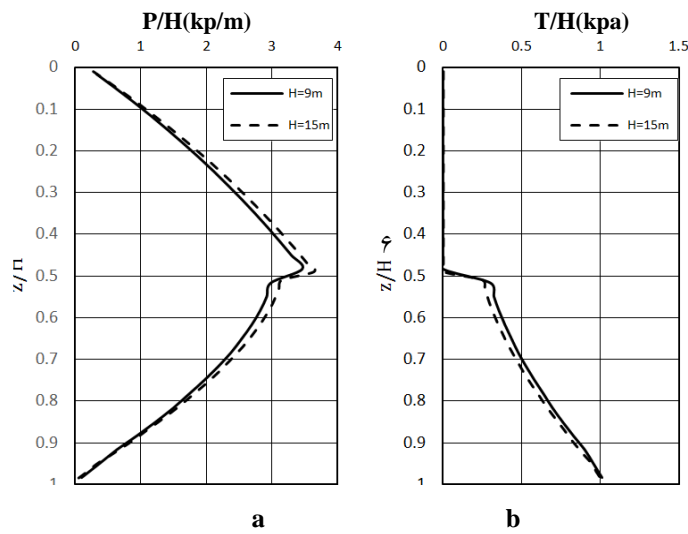


**Figure 7. Comparison of distribution of a) normalized lateral earth pressure on facing and b) normalized reinforcement's forces for different wall heights**

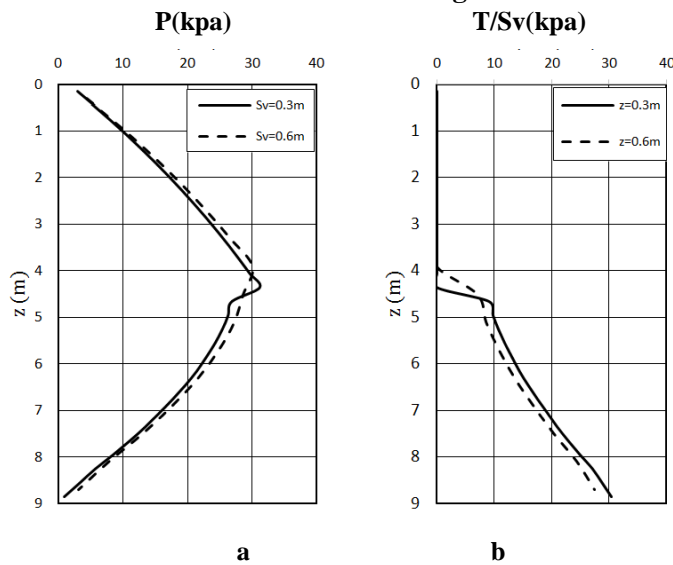


**Figure 8. Comparison of distribution of a) lateral earth pressure and b) mobilized tensile stress in reinforcements for different vertical spacing of reinforcements**

### 5. Comparison of reinforced and unreinforced backfills pressure

The applied earth pressures on facing from narrow reinforced and unreinforced backfills have been compared in Figure 9. The lateral earth pressure of unreinforced backfill was calculated using the horizontal slices formulation described in the preceding section with omitting the reinforcement force. The diagram of mobilized tensile stress in the reinforcements has also been presented in Figure 9. Since no force is mobilized in the reinforcements of upper layers, the lateral earth pressure diagrams are matched for the both reinforced and unreinforced backfills in upper part of the wall. Also, it can be observed that the earth pressure in upper part of the wall is almost equal to the seismic active earth pressure calculated by the well-known Mononobe-Okabe equation as follows:

$$P_{AE} = K_{AE} \gamma Z \quad (16)$$

$$= \frac{K_{AE} \cos^2(\varphi - \theta - \beta)}{\cos \theta \cos^2 \beta \cos(\delta + \beta + \theta) \left[ 1 + \sqrt{\frac{\sin(\varphi + \delta) \sin(\varphi - \theta - i)}{\cos(\delta + \beta + \theta) \cos(i - \beta)}} \right]} \quad (17)$$

$$\theta = \tan^{-1} \left( \frac{K_h}{1 - K_v} \right) \quad (18)$$

where  $\varphi$  is friction angle,  $\delta$  friction angle between backfill and wall surface,  $\beta$  slope of back of wall with respect to the vertical direction and  $i$  slope of backfill surface with respect to the horizontal direction.

In lower part of the reinforced backfill, the reinforcements start to carry the earth pressure gradually with depth and so a portion of the load is carried by the reinforcements. In fact, the total earth pressure is

divided between the facing and the reinforcements. As can be seen in Figure 9, if the tensile stress of reinforcements is added to the applied pressure on the facing, it will be closely equal to the lateral earth pressure of the unreinforced backfill. Another important point is that the summation of the lateral earth pressure and tensile stress of reinforcements is nearly constant with depth. These findings can be used to construct the diagram of earth pressure and reinforcements tension distribution in height of the wall.

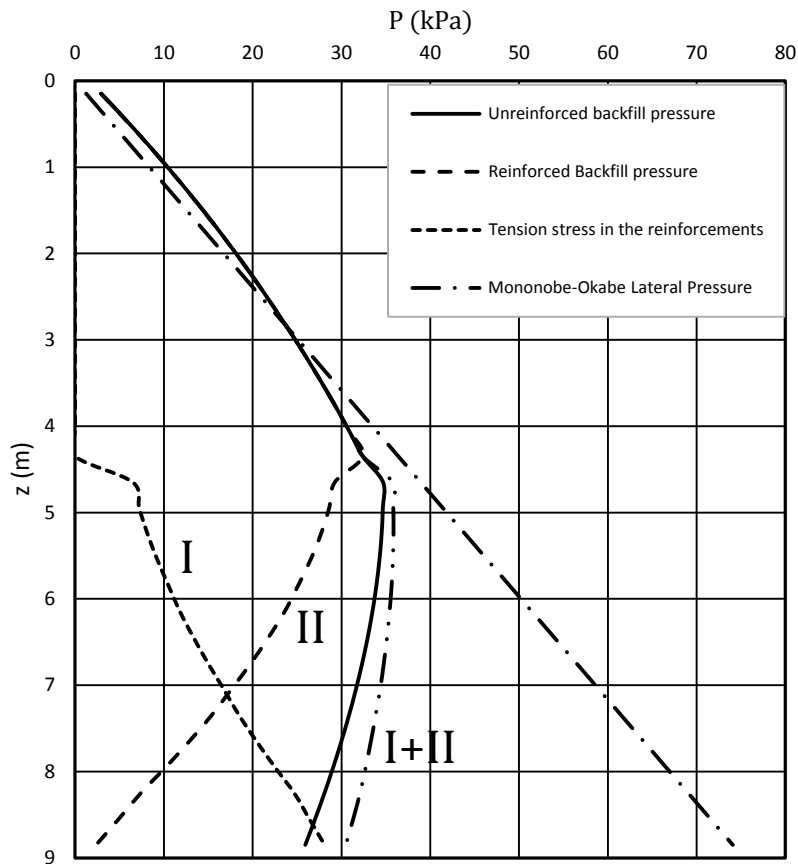


**Figure 9.** Effect of reinforcement on lateral earth pressure

## 6. Comparison of results with Mononobe-Okabe equation

The resultant thrust for the lateral earth pressures of different models that are presented in Figure 3 to 8, were calculated and compared to the thrust of the seismic active earth pressure obtained from the Mononobe-Okabe equation:

$$\sum P_{M.O.} = \frac{1}{2} K_{AE} \gamma H^2 \quad (19)$$

In Figure 10 the ratio of lateral earth thrust from horizontal slices method ( $\sum P_{H.S.M.}$ ) to Mononobe-Okabe equation ( $\sum P_{M.O.}$ ) was plotted versus the wall aspect ratio. It can be observed in this figure that the applied earth thrust on the facing decreases with increasing of the wall aspect ratio. As stated before, this observation is mainly related to the increase of reinforcements bonded length behind the failure wedge. As shown in Figure 10, the average of normalized lateral earth thrust varies from 0.53 to 0.34 by increasing of the wall aspect ratio from 0.3 to 0.5, respectively.

In the current design method, the facing is designed to support the active earth pressure developed in an unreinforced backfill [24]. However, Figure 10 indicates that the exerted pressure on the facing is significantly smaller than the active earth pressure of unreinforced backfill. Also, in the study of Ahmadabadi and Ghanbari [23] the lateral earth pressure in reinforced soil walls with unlimited backfill space was obtained less than %10 of the lateral earth pressure of unreinforced backfill which is due to the sufficient anchorage length of reinforcements. However, Figure 10 shows that in narrow backfills

owing to limited length of reinforcements, the pressure on the facing is considerably greater than the unlimited backfill.

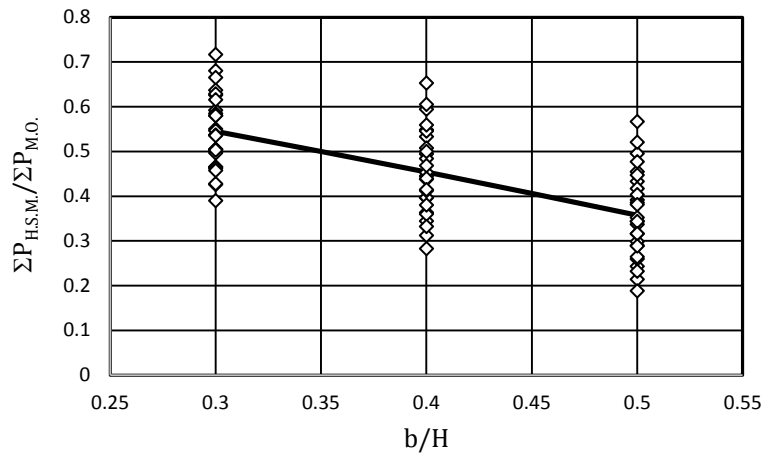


**Figure 10. Variation of ratio of lateral earth thrust from horizontal slices method to Mononobe-Okabe equation versus wall aspect ratio**

## Conclusion

In the current study, the seismic active earth pressure applied on the full-height rigid facing in the narrow geosynthetic-reinforced retaining walls with a stable rear surface was evaluated using limit equilibrium approach and horizontal slices method. The critical failure surface was assumed to extend linearly from the wall toe to the rear surface and then moves along the interface of the backfill and rear surface up to the backfill surface.

Because of the special shape of the failure wedge, the entire length of the upper reinforcements is placed inside the failure wedge and based on the limit equilibrium method, they not carry any load and

the soil pressure distribution is the same as the unreinforced backfill. The soil pressure in this part almost matches with the classical Mononobe-Okabe method. Below the intersection of the failure surface and rear wall, the reinforcements start to carry the earth pressure gradually with depth. By growing of the carried load by reinforcements, the applied pressure on the facing reduces until it reaches zero at the wall toe. The summation of the soil pressure and reinforcements tensile stress is nearly constant with depth and equal to the unreinforced backfill pressure.

By decreasing of the wall aspect ratio, the size of the lower part of the failure wedge and bonded length of the reinforcements decreases and consequently, the applied earth pressure on the facing increases. It was found that the ratio of resultant earth thrust to the Mononobe-Okabe equation is varying from 0.53 to 0.34 for the wall aspect ratio of 0.3 to 0.5, respectively.

### References

1. Rowe R. K., Ho S. K., "Horizontal deformation in reinforced soil walls", *Canadian Geotechnical Journal*, Vol. 35, No. 2 (1998) 312-327.
2. Shahgholi M., Fagher A., Jones C. J. F. P., "Horizontal slice method of analysis", *Geotechnique*, Vol. 51, No. 10 (2001) 881-885.
3. El-Emam M. M., Bathurst R. J., "Influence of reinforcement parameters on the seismic response of reduced-scale reinforced soil retaining walls", *Geotextiles and Geomembranes*, Vol. 25, No. 1 (2007) 33-49.



4. Nouri H., Fakher A., Jones C. J. F. P., "Development of horizontal slices method for seismic stability analysis of reinforced slopes and walls", *Geotextiles and Geomembranes*, Vol. 24 (2006) 175-187.
5. Nouri H., Fakher A., Jones C. J. F. P., "Evaluating the effects of the magnitude and amplification of pseudo-static acceleration on reinforced soil slopes and walls using the limit equilibrium horizontal slices method", *Geotextiles and Geomembranes*, Vol. 26, No. 3 (2008) 263-278.
6. Latha G. M., Krishna A. M., "Seismic response of reinforced soil retaining wall models: influence of backfill relative density", *Geotextiles and Geomembranes*, Vol. 26, No. 4 (2008) 335-349.
7. Yang G., Zhang B., Lv, P., Zhou Q., "Behaviour of geogrid reinforced soil retaining wall with concrete-rigid facing", *Geotextiles and Geomembranes*, Vol. 27, No. 5 (2009) 350-356.
8. Yang K. H., Kniss K. K., Zornberg J. G., Wright S. G., "Finite element analyses for centrifuge modeling of narrow MSE walls", *Proceedings of First Pan American Geosynthetics Conference, GEOAMERICAS 2008, Cancun, Mexico (2008)*.
9. Vieira C. S., Lopes M. L., Caldeira L. M., "Earth pressure coefficients for design of geosynthetic reinforced soil structures", *Geotextiles and Geomembranes*, Vol. 29, No. 5 (2011) 491-501.
10. Tatsuoka F., Murata O., Tateyama M., "Permanent geosynthetic-reinforced soil retaining walls used for railway embankments in Japan", *Proceedings of the International Symposium on Geosynthetic-Reinforced Soil Retaining Walls, Denver, Colorado, J. T. H., Wu (ed.) (1992) 101-130*.

11. Morrison K. F., Harrison F. E., Collin J. G., Dodds A., Arndt B., "Shored Mechanically Stabilized Earth (SMSE) wall systems", Federal Highway Administration, Report No. FHWA-CFL/TD-06-001 (2006).
12. Tatsuoka F., Tateyama M., Murata O., "Earth retaining wall with a short geotextile and a rigid facing", Proceedings of 12th ICSMFE, International Society of Soil Mechanics and Foundation Engineering, Volume 2 (1989) 1311-1314.
13. Murata O., Tateyama M., Tatsuoka F., Nakamura K., Tamura Y., "A reinforcing method for earth retaining walls using short reinforcing members and a continuous rigid facing", Proceedings of Geotechnical Engineering Congress, ASCE Geotechnical Special Publication 27 (1991) 935-946.
14. Woodruff R., "Centrifuge modeling of MSE-shoring composite walls", MSc. Thesis, University of Colorado, Boulder (2003).
15. Leshchinsky D., Hu Y., Han J., "Limited reinforced space in segmental retaining wall", Geotextiles and Geomembranes, Vol. 22, No. 6 (2004) 543-553.
16. Lawson C. R., Yee T. W., "Reinforced soil retaining walls with constrained reinforced fill zones", Proceedings of GeoFrontiers, ASCE Geo-Institute Conference (2005) 2721-2734.
17. Morrison K. F., Harrison F. E., Collin J. G., Anderson S. A., "Full-Scale testing of a shored mechanically-stabilized earth (SMSE) wall employing short reinforcements", ASCE Geotechnical Special Publication 165, Geosynthetics in Reinforcement and Hydraulic Applications (2007) 1-10.
18. Kniss K. K., Wright S., Zornberg J. G., Yang K. H., "Design considerations for MSE retaining walls constructed in confined spaces",

Center for Transportation Research (CTR), Report No. 0-5506-1, Austin, Texas (2007).

19. Lee Y. B., Ko H. Y., McCartney J. S., "Deformation response of shored MSE walls under surcharge loading in the centrifuge", *Geosynthetics International*, Vol. 17, No. 6 (2010).389-402.
20. Yang, K. H., Zornberg J. G., Hung W. Y., Lawson C. R., "Location of failure plane and design considerations for narrow geosynthetic reinforced soil wall systems", *Journal of GeoEngineering*, Vol. 6, No. 1 (2011) 27-40.
21. Koseki J., "Use of geosynthetics to improve seismic performance of earth structures", *Geotextiles and Geomembranes*, Vol. 34 (2012) pp.51-68.
22. Tatsuoka F., Tateyama M., Koseki J., Uchimura T., "Geotextile-reinforced soil retaining wall and their seismic behaviour", In: *Proceedings of the 10th Asian Regional Conference on S.M.F.E.*, Beijing, Vol. 2 (1995) 26-49.
23. Ahmadabadi M., Ghanbari A., "New procedure for active earth pressure calculation in retaining walls with reinforced cohesive-frictional backfill", *Geotextiles and Geomembranes*, Vol. 27 (2009) 456-463.
24. Horii K., Kishida H., Tateyama M., Tatsuoka F., "Computerized design method for geosynthetic-reinforced soil retaining walls for railway embankments", In: *Proceedings of Recent Case Histories of Permanent Geosynthetic-Reinforced Soil Retaining Walls*, Tokyo, Japan, Tatsuoka, F., Leshchinsky, D. (eds.) (1994) 205-218.

25. Azad A., Yasrobi S., Pak A., "Seismic active earth pressure distribution behind rigid retaining walls", *Soil Dynamics and Earthquake Engineering*, Vol. 28, No. 5 (2008) 365-375.
26. Shekarian S., Ghanbari A., Farhadi A., "New seismic parameters in the analysis of retaining walls with reinforced backfill", *Geotextiles and Geomembranes*, Vol. 26 (2008) 350-356.
27. Ghanbari A., Ahmadabadi M., "Pseudo-dynamic active earth pressure analysis of inclined retaining walls using horizontal slices method", *Scientia Iranica, Transaction A: Civil Engineering*, Vol. 17, No. 2 (2010) 118-130.
28. Ghanbari A., Taheri M., "An analytical method for calculating active earth pressure in reinforced retaining walls subject to a line surcharge", *Geotextiles and Geomembranes*, Vol. 34 (2012) 1-10.
29. Janssen H. A., "Versuche über Getreidedruck in Silozellen", *Zeitschrift des Verein Deutscher Ingenieure*, Vol. 39 (1895) 1045-1049.